Int. J. Heat Mass Transfer. Vol. 21, pp. 455–465. Pergamon Press 1978. Printed in Great Britain

UNSTEADY STATE MASS TRANSFER THROUGH THE INTERFACE OF SPHERICAL PARTICLES—II

DISCUSSION OF RESULTS OBTAINED BY THEORETICAL METHODS*

H. BRAUER
Institut für Chemieingenieurtechnik, Technische Universität, Berlin, Germany

(*Received* 11 *October* 1976 *and in revised form* 16 *August* 1977)

Abstract—In the second part of the investigation the results obtained by numerical solution of the differential equations given in the first part are thoroughly discussed. The discussion starts with mass transfer through the particle interface when there is no movement in either phase. It is limited to the mean concentration in the sphere and the mean Sherwood numbers for both phases. Empirical equations are presented for the mean concentration in the sphere for the limiting cases of mass-transfer resistance in one of the two phases only. The last chapter of the paper contains the discussion pertaining to the influence of convection on mass transfer. With mass-transfer resistance in the sphere only there exists an upper limit for the mean Sherwood number which is due to the fact that the streamlines inside the sphere become lines of constant concentration. The instantaneous Sherwood number changes stepwise with time which may be explained by the movement of fluid elements in the sphere. For the second limiting case, mass transfer resistance in the surrounding fluid only, the mean Sherwood number is discussed as a function of the Fourier-, Henry-, and convection-number.

1. INTRODUCTION

IN THIS paper, which is the second part of a comprehensive theoretical investigation of unsteady state mass transfer through the interface of spherical particles, a comprehensive discussion of the results obtained is presented. The physical phenomena of the mass-transfer process as well as the underlying differential equations and boundary conditions are presented in Part I of the investigation.

2. ANALYTICAL SOLUTIONS FOR LIMITING CONDITIONS OF THE FOURIER NUMBER

For the two cases, $Fo_m \to 0$ and $Fo_m \to \infty$, the differential equations for the concentration field may be simplified in such a way, that analytical solutions may be obtained [1, 2]. The resulting equations will be repeated here because they are helpful in the discussion of numerical results.

2.1. *Analytical solutions for* $Fo_m \to 0$

For $Fo_{m2} = Fo_{m1} = Fo_m \to 0$ concentration changes occur in the immediate vicinity of the interface only. In this case the convection has no influence at all on the mass-transfer process. This is the reason why the following equations are of fundamental importance.

The equations for the mean instantaneous Sherwood numbers pertaining to phase 1 and 2:

$$Sh_{1t} = \frac{2/\sqrt{\pi}}{\left(\frac{D_1}{D_2}\right)^{1/2} + H^* \frac{D_1}{D_2}} Fo_{m2}^{-1/2} = \frac{2/\sqrt{\pi}}{1 + H^* \left(\frac{D_1}{D_2}\right)^{1/2}} Fo_{m1}^{-1/2} \quad (1)$$

$$Sh_{2t} = \frac{2/\sqrt{\pi}}{H^* + \left(\frac{D_2}{D_1}\right)^{1/2}} Fo_{m2}^{-1/2}. \quad (2)$$

The equations for the time mean value of the Sherwood numbers pertaining to phase 1 and 2:

$$Sh_1 = 2Sh_{1t}, \quad (3)$$

$$Sh_2 = 2Sh_{2t}. \quad (4)$$

These equations apply for the general case of arbitrary distribution of mass-transfer resistance in the two phases concerned.

For the special case, that mass-transfer resistance occurs in phase 1 (sphere) only, one obtains from equation (3) observing $H^*(D_1/D_2)^{1/2} \to 0$:

$$Sh_1 = \frac{4/\sqrt{\pi}}{Fo_{m1}^{1/2}}. \quad (5)$$

The Sherwood number depends on the Fourier number only. The Henry number H^* and the ratio of diffusion coefficients have no influence on Sh_1. According to Figs. 2 and 3 of Part I the concentration in the interface is zero for all values of Fo_{m1}. From equation (5) one obtains the following equation for the mass-transfer coefficient:

$$\beta = \frac{2}{\sqrt{\pi}} \left(\frac{D_1}{t}\right)^{1/2}. \quad (6)$$

It is to be noted that for $t \to 0$ the mass-transfer coefficient is independent of particle diameter d_p. For the other special case with mass-transfer resistance in phase 2 (surrounding fluid) only the condition $H^*(D_1/D_2)^{1/2} \to \infty$ leads from equation (4) to the result:

$$Sh_2 = \frac{4/\sqrt{\pi}}{H^*} \frac{1}{Fo_{m2}^{1/2}}. \quad (7)$$

*For nomenclature see Part I of this paper.

The influence of H^* is due to the fact, shown in Figs. 4 and 5 of Part I, that the concentrations in the interface are always greater than zero.

2.2. *Analytical solution for* $\mathrm{Fo_m} \to \infty$

For $Fo_{m1} = Fo_{m2} = Fo_m \to \infty$ the state of equilibrium is reached. The local concentrations are independent of radial coordinate. For this case a simple mass balance leads to the results:

$$Sh_1 = \frac{2/3}{Fo_{m1\infty}}, \tag{8}$$

$$Sh_2 = \frac{2/3}{Fo_{m2\infty}}. \tag{9}$$

From these equations the following equation for the mass-transfer coefficient may be derived:

$$\beta = \frac{1}{6}\frac{d_p}{t}. \tag{10}$$

For $t \to \infty$ the mass-transfer coefficient is a linear function of the particle diameter d_p.

3. DISCUSSION OF SOME NUMERICAL RESULTS FOR MASS TRANSFER IN A MOTIONLESS SYSTEM

Mass transfer through the interface of a spherical particle with fluid motion in one or even both phases is an extremely complicated process. It seems therefore advisable to use the simple case of mass transfer in a motionless system as introduction.

3.1. *Mean concentration in sphere*

The mean concentration in the sphere alters between the limiting values $\bar{\xi}_1 = 0$ and $\bar{\xi}_1 = 1$ while the mean concentration in the surrounding fluid is according to definition always $\bar{\xi}_2 = 0$. This is the reason, why attention is paid to $\bar{\xi}_1$ only.

For the condition of mass-transfer resistance in the sphere only, that is $H^*(D_1/D_2)^{1/2} \to 0$, the mean concentration is shown in Fig. 1. It is a function of Fo_{m1} only. With mass-transfer resistance in the sphere only, the following condition is met:

$$H^*\left(\frac{D_1}{D_2}\right)^{1/2} \to 0, \text{ with } H^* < 1 \text{ and } D_1/D_2 < 1.$$

For the other limiting case with mass-transfer resistance in the surrounding fluid only, that is $H^*(D_1/D_2)^{1/2} \to \infty$, the mean concentration $\bar{\xi}_1$ is according to Fig. 2 a function of Fo_{m2} and H^*. With mass-transfer resistance in phase 2 only, the prevailing condition is as follows:

$H^*(D_1/D_2)^{1/2} \to \infty$, with $H^* > 1$ and $D_1/D_2 > 1$.

With increasing value of the Henry number H^* the mean concentration in the sphere decreases more slowly with time than for smaller values of H^*.

3.2. *Mean Sherwood number*

For mass-transfer resistance in the sphere only, the mean Sherwood number Sh_1 is given in Fig. 3. Curve *a* gives the numerically established relation between Sh_1 and Fo_{m1} over the whole range of Fo_{m1}, while curve *b* represents equation (8) for $Fo_{m1} \to \infty$ and curve *c* equation (5) for the other limiting case with $Fo_{m1} \to 0$.

Figure 4 gives the numerical results for the case of mass-transfer resistance in the surrounding fluid only. Curve *b* represents equation (9) for $Fo_{m2} \to \infty$. For $Fo_{m2} \to 0$ the curves may be calculated by means of equation (7). The success achieved by the mass transfer through the interface may be easily judged by means of the curves for $\bar{\xi}_1 = \text{const}$. Curve *b* is according to equation (18) of Part I together with equation (9) equivalent to $\bar{\xi}_1 = 0$.

3.3. *Empirical equations*

The application of the numerical results presented will be considerably facilitated by empirical equations developed for the mean concentration $\bar{\xi}_1$. These equations may be used to calculate the transferred mass M_A by means of equation (17) of Part I.

3.3.1. *Mass-transfer resistance in the sphere only.* The empirical equations set up for this case are as follows:

Low Fo_{m1} region:

$$\bar{\xi}_1 = 1 - \frac{3.935 Fo_{m1}^{1/2}}{1 + 0.30 Fo_{m1}^{-0.012}}. \tag{11}$$

Range of application

$$0 \leqslant Fo_{m1} \leqslant 4 \times 10^{-2}$$
$$0.43 \leqslant \bar{\xi}_1 \leqslant 1.0$$

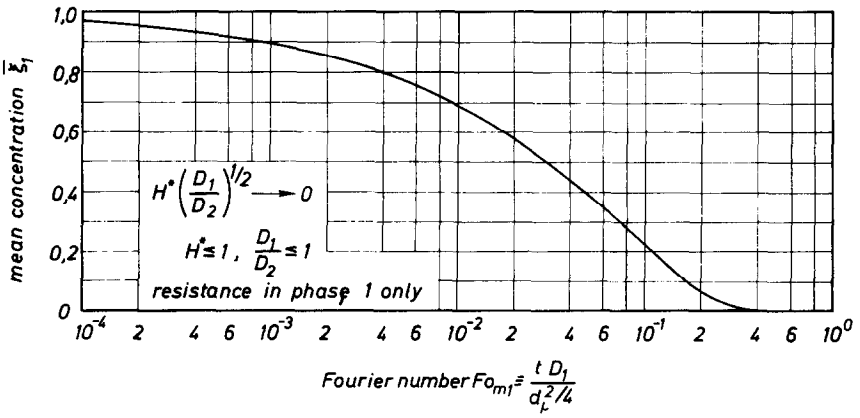

FIG. 1. Mean concentration in sphere for the limiting case of resistance in the sphere only.

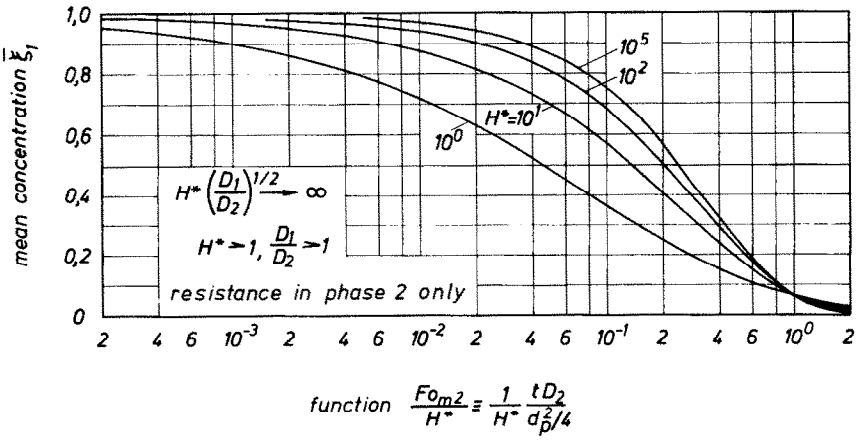

FIG. 2. Mean concentration in sphere for the limiting case of resistance in the surrounding fluid only.

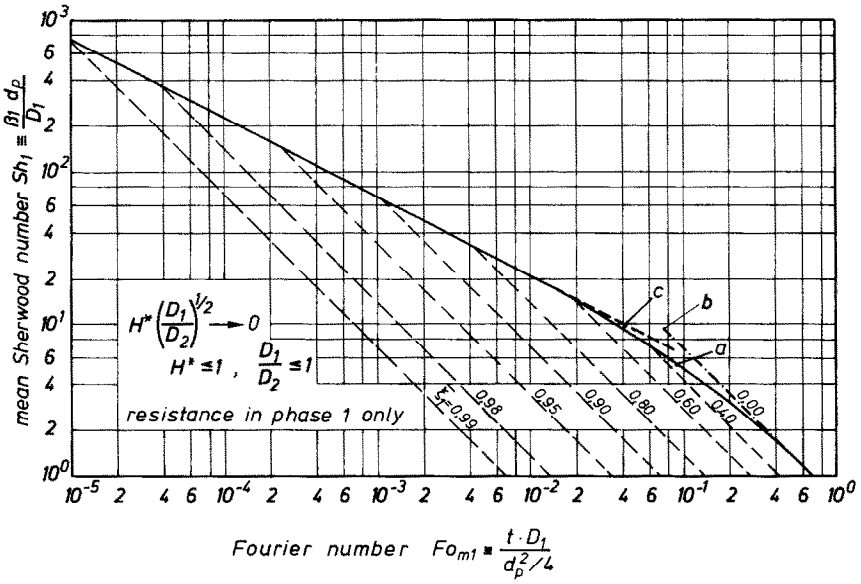

FIG. 3. Mean Sherwood number Sh_1 for the limiting case of resistance in the sphere only. Curve *a* represents numerical results, curve *b* equation (59) and curve *c* equation (56).

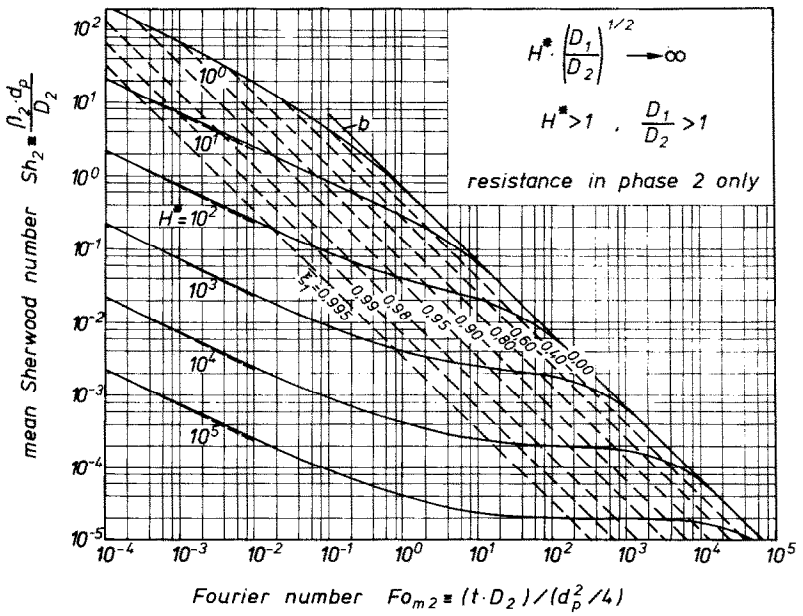

FIG. 4. Mean Sherwood number Sh_2 for the limiting case of resistance in the surrounding fluid only. Curve *b* represents equation (60).

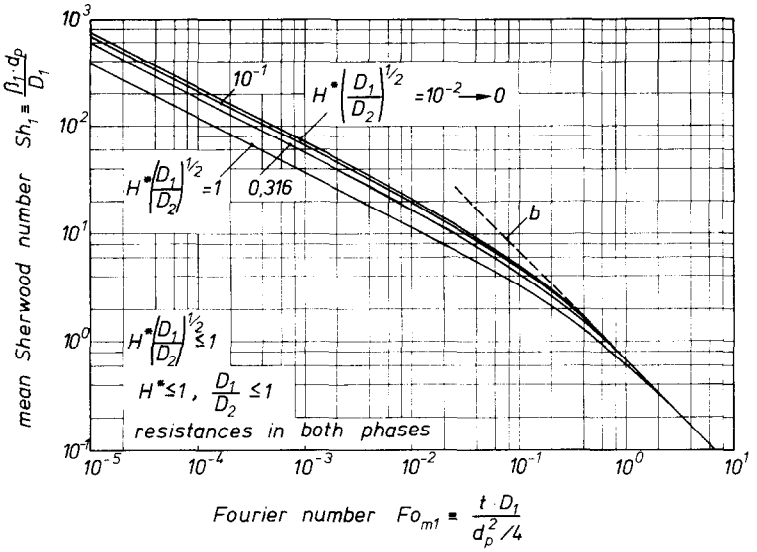

FIG. 5. Mean Sherwood number Sh_1 for the general case of resistances in both phases. Curve b represents equation (59).

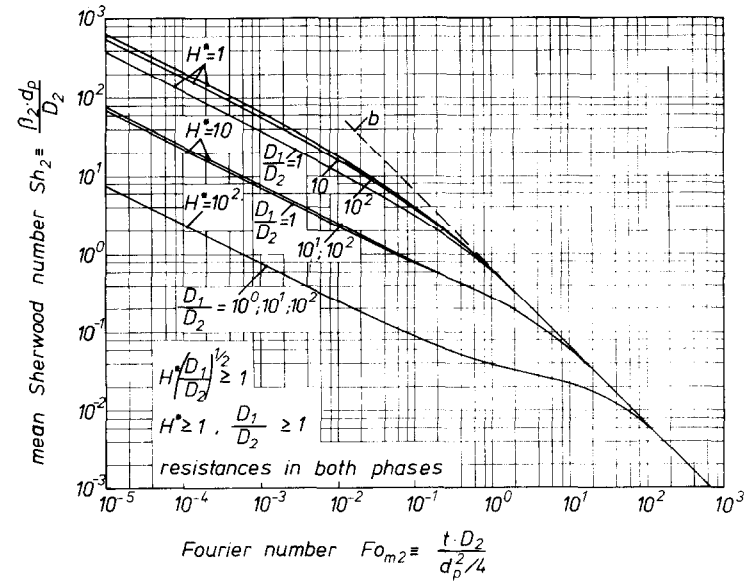

FIG. 6. Mean Sherwood number Sh_2 for the general case of resistances in both phases. Curve b represents equation (60).

Maximum error: $\pm 3.8\%$

High Fo_{m1} region:

$$\bar{\xi}_1 = 0.646 \exp(-10.15 Fo_{m1}). \tag{12}$$

Range of application:

$$4 \times 10^{-2} \leq Fo_{m1} \leq \infty$$
$$0 \leq \bar{\xi}_1 \leq 0.43$$

Maximum error: $\pm 3.8\%$.

Combining equations (18) of Part I and (12) the mean Sherwood number Sh_1 may be calculated with a maximum error of 1.2%. If the Sherwood number in the low Fo_{m1} region is desired application of the analytical equation (5) is suggested.

3.3.2. *Mass-transfer resistance in the surrounding fluid only.* For this case the mean concentration $\bar{\xi}_1$ is a function of the Fourier number Fo_{m2} and the Henry number H^*. The equations developed for this case are consequently more complicated than those for the other limiting case.

An equation of rather general importance is the following:

$$\bar{\xi}_1 = \frac{1}{\left\{1 + \left[\left(\frac{Fo_{m2}}{n}\right)^m\right]^p\right\}^{1/p}}. \tag{13}$$

The values of m, n and p are functions of the Henry number H^*, they are given in Table 1 together with the maximum relative error in $\bar{\xi}_1$. Equations for m, n and p

Table 1. Values of m, n, and p as functions of H^* as well as maximum relative errors for $\bar{\xi}_1$ in two ranges of $\bar{\xi}_1$

H^*	m	n	p	Maximum relative error of $\bar{\xi}_1$ in % range $0.1 \leqslant \bar{\xi}_1 \leqslant 1$	range $0.05 \leqslant \bar{\xi}_1 \leqslant 1$
1	1.12	12.3×10^{-2}	0.600	5.3	14
2	1.28	37.0×10^{-2}	0.570	5.9	15
4	1.47	1.0×10^{0}	0.541	7.4	16
10^1	1.80	3.4×10^{0}	0.500	6.9	20
10^2	2.70	5.3×10^{1}	0.425	7.4	18
10^3	2.96	5.5×10^{2}	0.425	7.4	18
10^4	3.10	5.6×10^{3}	0.430	6.9	7

have been set up too and are as follows:

$1 \leqslant H^* \leqslant 10^2$:

$$\left.\begin{aligned} m &= 1.12H^{*0.197} \\ p &= 0.6/H^{*0.0748} \\ &n \text{ in the range } 1 \leqslant H^* \leqslant 10: \\ n &= -1.22 \times 10^{-3}H^{*3} + 3.12 \times 10^{-2}H^{*2} \\ &\quad + 1.62 \times 10^{-1}H^* - 6.89 \\ &n \text{ in the range } 10^1 \leqslant H^* \leqslant 10^2 \\ n &= 1.51 \times 10^{-3}H^{*2} + 0.387H^* - 0.573. \end{aligned}\right\} \quad (14)$$

$10^2 \leqslant H^* \leqslant 10^4$:

$$\left.\begin{aligned} m &= 2.48H^{*0.0254} \\ n &= 0.533H^* \\ p &= 0.414H^{*4.35 \times 10^{-3}}. \end{aligned}\right\} \quad (15)$$

For the range $10^4 \leqslant H^* \leqslant 10^5$ and $0.05 \leqslant \bar{\xi}_1 \leqslant 1$ the following equation has been set up:

$$\bar{\xi}_1 = \exp(-2.76Fo_{m2}/H^*). \quad (16)$$

3.4. *Some remarks on mass transfer with resistances in both phases*

With mass-transfer resistances in both phases the Sherwood number Sh_1 is according to equation (1) a function of Fo_{m1} and the product $H^*(D_1/D_2)^{1/2}$, while Sh_2 is according to equation (2) a function of Fo_{m2}, H^* and D_1/D_2. Some of the results obtained are presented in Figs. 5 and 6, that have already been published [1, 2].

4. DISCUSSION OF SOME NUMERICAL RESULTS FOR MASS TRANSFER WITH FLUID MOTION

In most cases of practical importance the involved fluids are in a state of motion. The influence of fluid motion on mass transfer will be discussed in this chapter. It should be kept in mind though, that for the two limiting cases of $Fo_m \to 0$ and $Fo_m \to \infty$ motion looses its influence.

4.1. *Mass-transfer resistance in the sphere only*

4.1.1. *Local and mean concentration.* With mass-transfer resistance in the sphere only, the local dimensionless concentration in the surrounding fluid is $\xi_2 = \xi_{2p} = \xi_{1p} = 0$, while the local concentration inside the sphere ξ_1 is given by:

$$\xi_1 = f_1[r^*; Fo_{m1}; (ReSc)_2; \eta^*]. \quad (17)$$

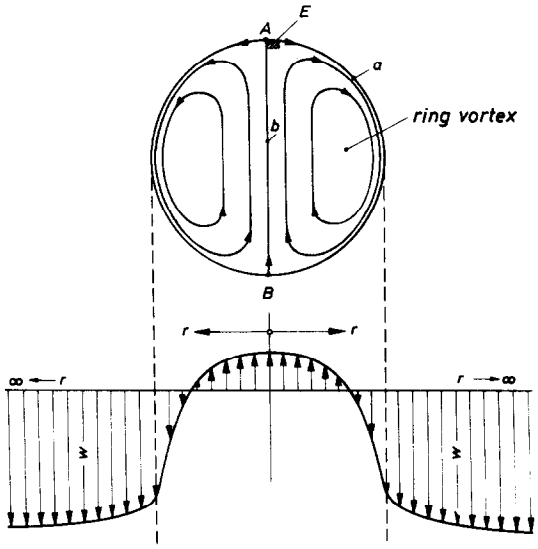

FIG. 7. Fluid motion inside and outside the sphere.

With creeping flow conditions, $Re \to 0$, this function simplifies to:

$$\xi_1 = f_2\left[r^*; Fo_{m1}; \frac{(ReSc)_2}{1+\eta^*}\right]. \quad (18)$$

In these functions $\eta^* \equiv \eta_1/\eta_2$ is the ratio of the viscosity of the two fluids involved. The fluid motion inside and outside the sphere is given in a qualitative way in Fig. 7.

The local concentration as it changes with time is shown in Fig. 8(a–c). The convection number, $(ReSc)_2/(1+\eta^*) = 10^3$, is kept constant. The Fourier number Fo_{m1} is 2.25×10^{-3} in Fig. 8(a), 8.1×10^{-3} in Fig. 8(b), and 2.2×10^{-2} in Fig. 8(c). With increasing Fourier number the local concentration decreases from $\xi_1 = 1$ at $Fo_{m1} = 0$ to $\xi_1 = 0$ at $Fo_{m1} = \infty$. Concentration changes start at low values of Fo_{m1} near the spherical interface; they are more pronounced at the backward stagnation point at $\theta = 180°$ than at the forward stagnation point at $\theta = 0°$, which is due to the fluid motion inside the sphere. In Fig. 7 the movement of element E from the forward point A to the backward stagnation point (point B) parallel to the interface may be pursued following the arrowed line. After arriving at point B the element moves through the axis of the sphere to the forward stagnation point A. This movement through the axis leads to a kind of concentration tunnel within the sphere. It is to be clearly seen in Figs. 8(b) and (c).

The mean concentration $\bar{\xi}_1$ in the sphere is given in Fig. 9 as a function of Fo_{m1} for several values of the convection number $(ReSc)_2/(1+\eta^*)$. The calculations for $(ReSc)_2/(1+\eta^*) \to \infty$ have been carried out by Carrubba [3]. The results of Carrubba differ from those presented by Kronig and Brink [4] which are based on an analytical solution of an incomplete differential equation.

The lower limit for $\bar{\xi}_1$ is given by the curve for $(ReSc)_2/(1+\eta^*) \to \infty$. The lower limiting curve is due to the fact, that the streamlines in the sphere have

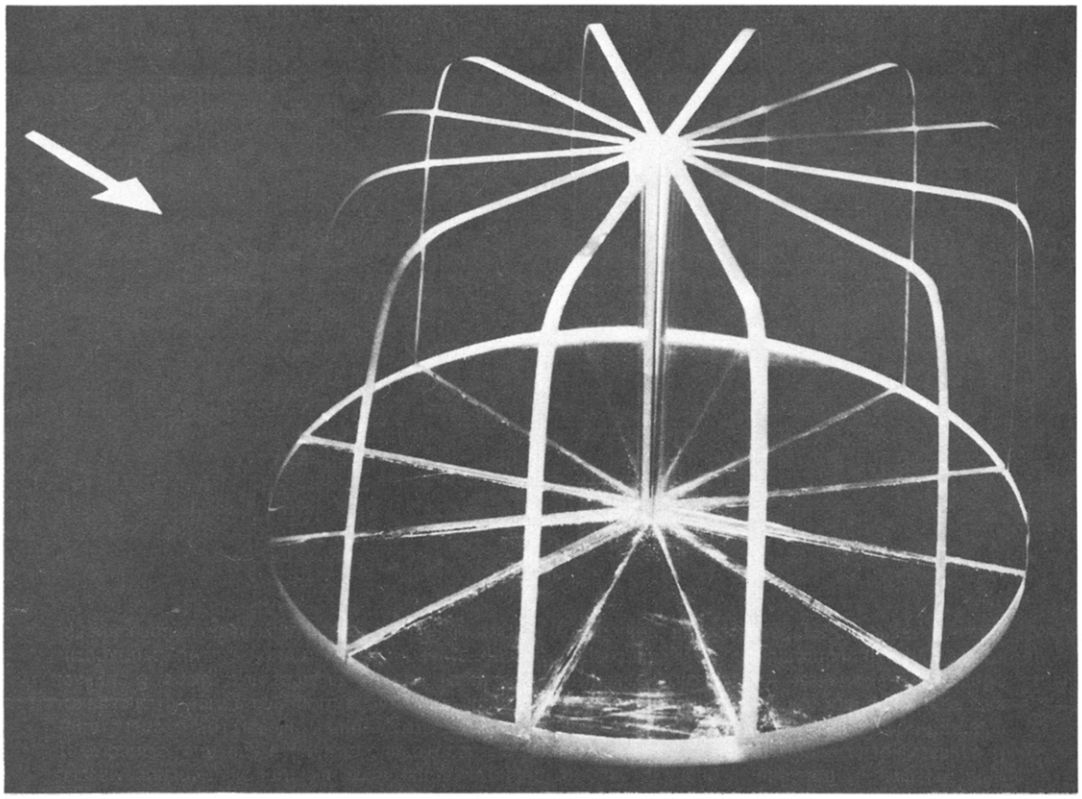

Fig. 8(a): $Fo_{m1} = 2.25 \times 10^{-3}$ and $\xi_1 = 0.84$

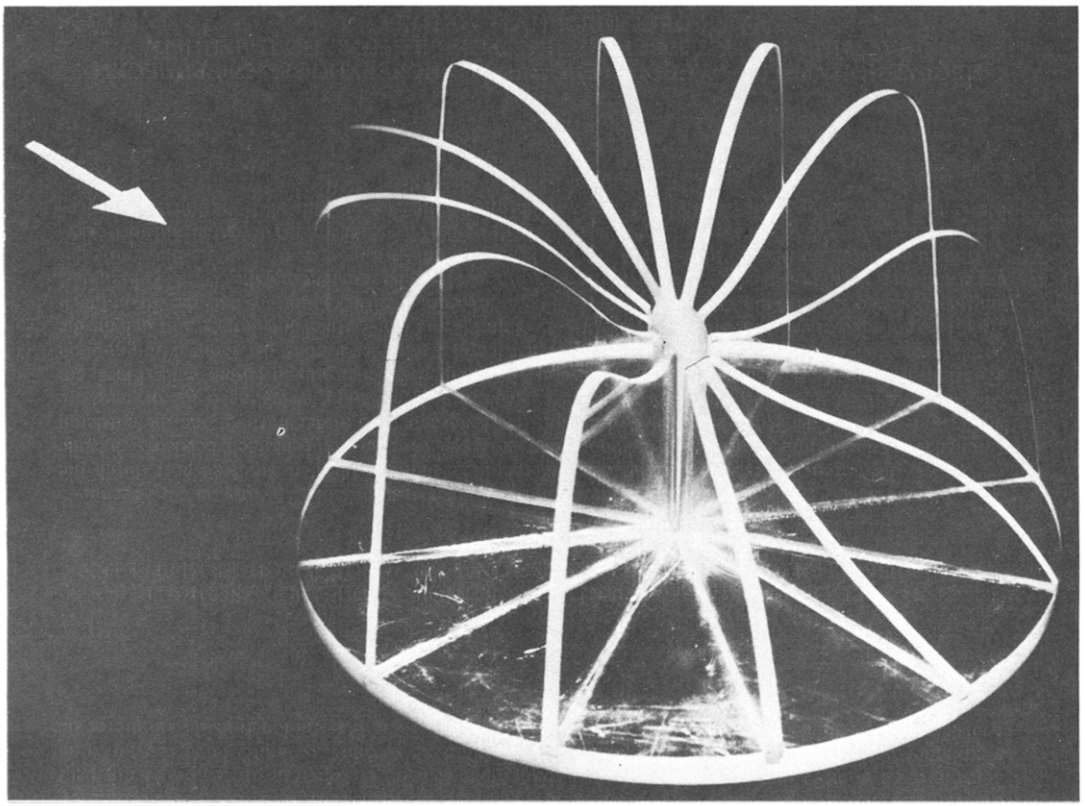

Fig. 8(b): $Fo_{m1} = 8.10 \times 10^{-3}$ and $\xi_1 = 0.67$

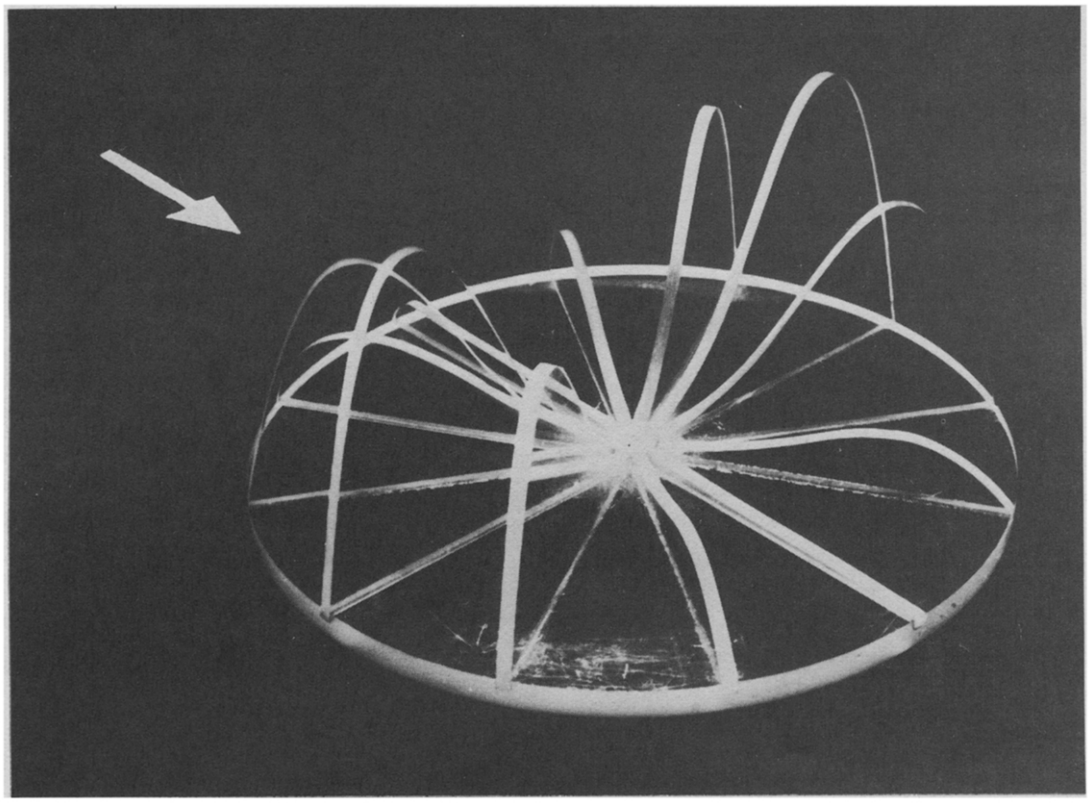

Fig. 8(c): $Fo_{m1} = 2.20 \times 10^{-2}$ and $\bar{\xi}_1 = 0.38$.

FIG. 8. Concentration field within the sphere for the limiting case of resistance in the sphere only

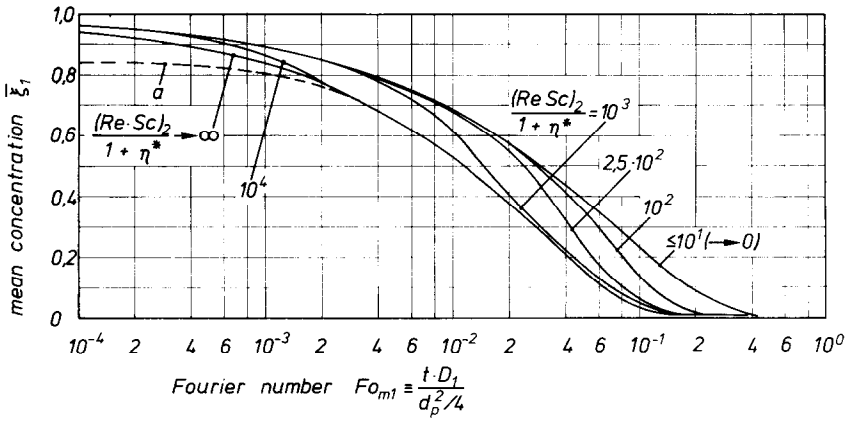

FIG. 9. Mean concentration in sphere with fluid motion in both phases for the special case of resistance in the sphere only.

become lines of constant concentration. This happens when the conductive transport normal to the streamlines is negligibly small compared with the convective transport in the direction of the streamlines. The curve for $(ReSc)_2/(1+\eta^*) \to \infty$ may be represented by the following equations:

Low Fo_{m1} region:

$$\bar{\xi}_1 = 1 - 4.546 Fo_{m1}^{1/2}. \tag{19}$$

Ranges of application:

$$0 \leqslant Fo_{m1} \leqslant 1.57 \times 10^{-2}$$
$$0.43 \leqslant \bar{\xi}_1 \leqslant 1.0$$

Maximum error: $\pm 3.6\%$.

High Fo_{m1} region:

$$\bar{\xi}_1 = 0.7 \exp(-31 Fo_{m1}). \tag{20}$$

Ranges of application:

$$1.57 \times 10^{-2} \leqslant Fo_{m1} \leqslant \infty$$
$$0 \leqslant \bar{\xi}_1 \leqslant 0.43$$

Maximum error: $\pm 1\%$.

The equations available for the two limiting cases, $(ReSc)_2/(1+\eta^*) \to 0$ and $\to \infty$, form a sound basis for mass-transfer calculations when convection is either present or not. For all values of $(ReSc)_2/(1+\eta^*) \geqslant 10^4$ it is always permissible to make use of equations (19) and (20).

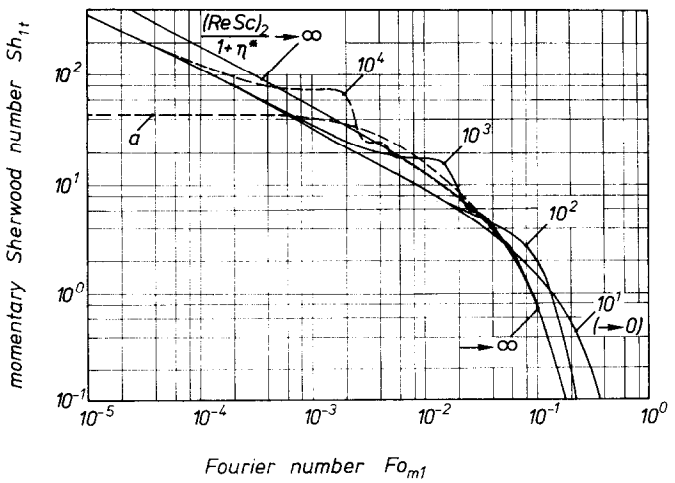

FIG. 10. Instantaneous Sherwood number Sh_{1t} for the limiting case of resistance in the sphere only as a function of Fo_{m1} for several values of the convection number $(ReSc)_2/(1+\eta^*)$. Curve *a* after Kronig and Brink.

The upper limit for $\bar{\xi}_1$ is given by the curve for $(ReSc)_2/(1+\eta^*) \to 0$. This curve is identical with the one given in Fig. 1; equations (11) and (12) describe this curve. In this case convective transport in the sphere may be neglected. Mass transfer is due to molecular transport only.

4.1.2. *Instantaneous and mean Sherwood number.* The instantaneous Sherwood number Sh_{1t} has been defined by equation (45) of Part I. In Fig. 10 Sh_{1t} is presented as a function of Fo_{m1} for several values of the convection number $(ReSc)_2/(1+\eta^*)$. There are again two limiting curves for $(ReSc)_2/(1+\eta^*) \to \infty$ and $\to 0$. Curve *a* has been presented by Kronig and Brink [4]. It is correct for $Fo_{m1} \to \infty$ only. At low values of Fo_{m1} all curves in Fig. 10 start off from the one for $(ReSc)_2/(1+\eta^*) \to 0$ and coincide with the curve for $(ReSc)_2/(1+\eta^*) \to \infty$ at high values of Fo_{m1}. The characteristic features of the curves are the steps. There are ranges in which Sh_{1t} is almost independent of Fo_{m1} alternating with ranges, in which Sh_{1t} is an extremely strong function of Fo_{m1}. The cause for the stepwise change of Sh_{1t} has been carefully investigated by Schmidt-Traub [5] and Carrubba [3].

The steps are due to the fluid movement in the sphere. Figure 11 shows the positions of the fluid elements *A*, *B*, *C* and *D* at two different values of Fo_{m1}. The elements are moving along the interface and the axis of the sphere. The movement starts at $Fo_{m1} = 0$ with element *A* in the forward stagnation point according to Fig. 11(a). According to the initial condition the local concentration is $\bar{\xi}_{10} = 1$.

In the first time interval the elements *A* and *B* move along the interface; element *B* vanishes at the backward stagnation point into the interior of the sphere. The concentration of these elements decreases while they move along the interface. In the same time interval the elements *D* and *C* move along the axis of the sphere and get into the interface. The end of the first time interval is reached, when element *C* reaches the forward stagnation point according to Fig. 11(b). During the first time interval the concentration of all fluid elements of the sphere reaching the forward

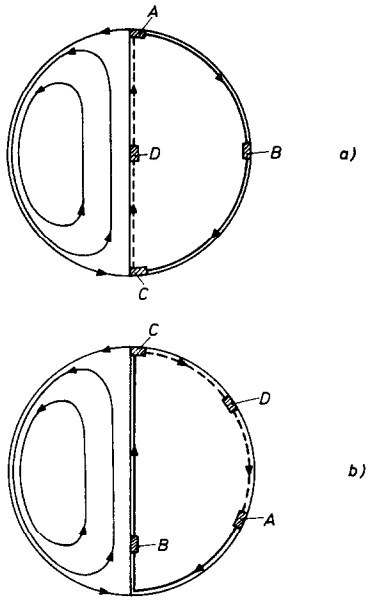

FIG. 11. Movement of fluid elements *A*, *B*, *C* and *D* inside the spherical particle.

stagnation point is $\bar{\xi}_1 = \bar{\xi}_{10} = 1$. This is the reason why the instantaneous Sherwood number approaches a constant value.

The second time interval starts with element *C* leaving the forward stagnation point and moving along the interface. All fluid elements reaching in the second interval the forward stagnation point have a lower concentration. The result is a steep decrease of Sh_{1t}. The end of the second interval has come when element *A* reaches the forward stagnation point again. The cycle then starts anew, but a less pronounced step will be the result because all elements will have a decreasing concentration.

The mean Sherwood number Sh_1 is shown in Fig. 12 as a function of Fo_{m1} for several values of the convection number $(ReSc)_2/(1+\eta^*)$. The first step in the curves for Sh_{1t} are still to be found in the curves for Sh_1. The following steps are levelled off though.

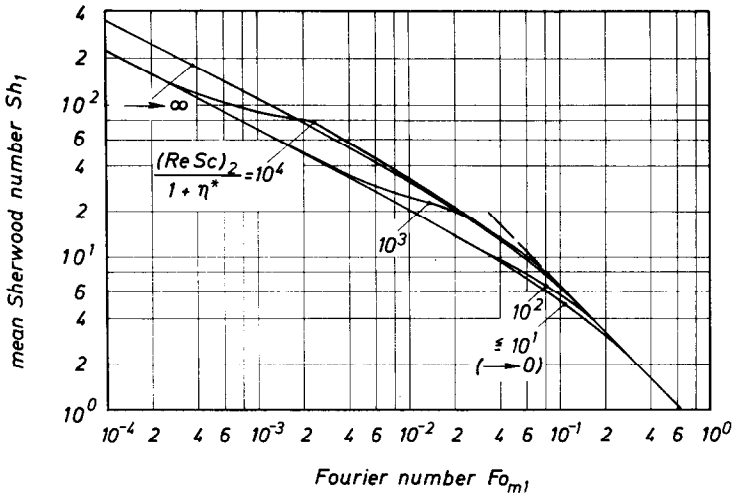

FIG. 12. Mean Sherwood number Sh_1 for the limiting case of resistance in the sphere only as a function of Fo_{m1} for several values of the convection number $(ReSc)_2/1+\eta^*)$.

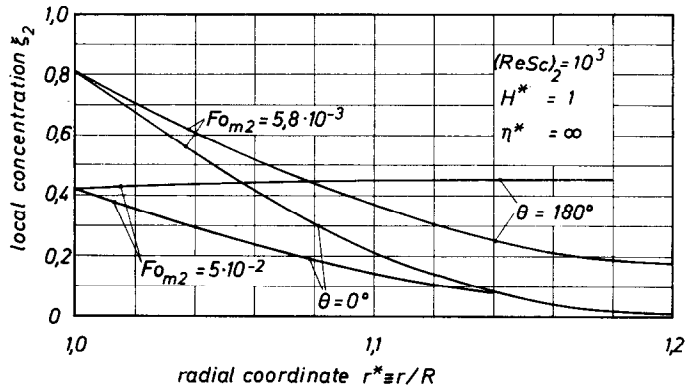

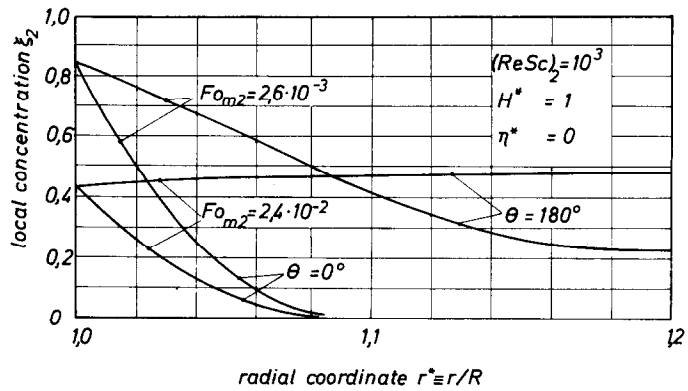

FIGS. 13 and 14. Local concentration ξ_2 in surrounding fluid for the limiting case of resistance in the surrounding fluid only:
Fig. 13: $\eta^*=\infty$, particle with rigid interface:
Fig. 14: $\eta^*=0$, particle with ideal mobility of interface.

4.2. *Mass-transfer resistance in the surrounding fluid only*

4.2.1. *Local and mean concentration.* With mass-transfer resistance in the surrounding fluid only the local concentration in the sphere is independent of the radius r^* and equal to the concentration in the interface:

$$\xi_1=\bar{\xi}_1=\xi_{1p}=\xi_{2p}. \tag{21}$$

The mean concentration $\bar{\xi}_1$ is given by the function:

$$\bar{\xi}_1=f_1[Fo_{m2};H^*;(ReSc)_2;\eta^*]. \tag{22}$$

The local concentration in the surrounding fluid ξ_2 is given by the following function:

$$\xi_2=f_2[r^*;Fo_{m2};H^*;(ReSc)_2;\eta^*]. \tag{23}$$

In Figs. 13 and 14 the local concentration ξ_2 is shown for $\eta^*=\infty$ and $\eta^*=0$ with $H^*=1$ and

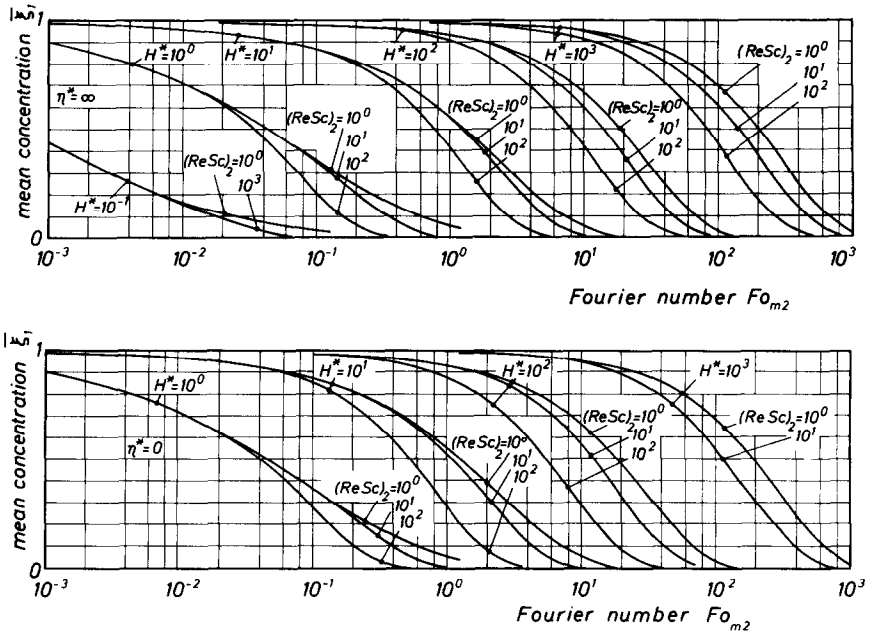

FIGS. 15 and 16. Mean concentration in sphere for the special case of resistance in the surrounding fluid only:
Fig. 15: $\eta^* = \infty$, particle with rigid interface:
Fig. 16: $\eta^* = 0$, particle with ideal mobility of interface.

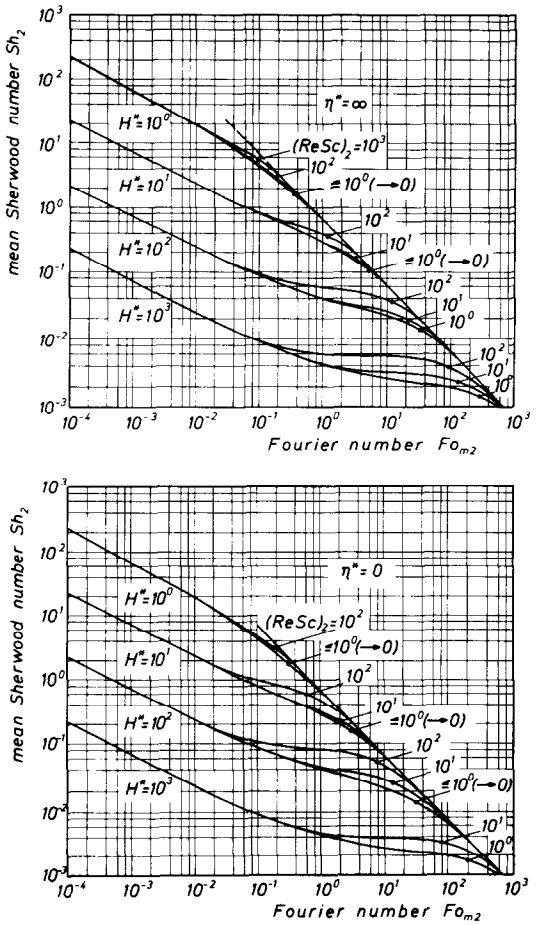

FIGS. 17 and 18. Mean Sherwood number Sh_2 for the limiting case of resistance in the surrounding fluid only:
Fig. 17: $\eta^* = \infty$, particle with rigid interface:
Fig. 18: $\eta^* = 0$, particle with ideal mobility of interface.

$(ReSc)_2 = 10^3$ kept constant for both cases. Curves are presented for two values of Fo_{m2} and angle θ. It may be of interest to note that the local concentration ξ_2 for $\theta = 180°$ is increasing slightly over a limited range of r^* instead of decreasing. This proves that there are limited time intervals during which the mass transfer in the vicinity of the backward stagnation point is directed contrary to the general direction. The concentration gradient in the interface is steeper for $\eta^* = 0$ than for $\eta^* = \infty$ because of the fluid motion within the sphere.

The mean concentration in the sphere $\bar{\xi}_1$ is shown in Figs. 15 and 16 for $\eta^* = \infty$ and $\eta^* = 0$. With increasing Henry number the influence of the convection number $(ReSc)_2$ is felt already at a higher concentration.

4.2.2. *Mean Sherwood number.* The mean Sherwood number Sh_2 is given for $\eta^* = \infty$ and $\eta^* = 0$ in Figs. 17 and 18. The curves given for $(ReSc)_2 \leqslant 10°$ coincide with those given in Fig. 4 for the motionless system. It is important to note that the influence of the convection number increases slowly with increasing Henry number H^*. As a first approximation the influence of $(ReSc)_2$ may be neglected, when $H^* < 10^1$. But even for higher values of H^* the results discussed for motionless systems will always give a sound basis for mass-transfer calculations.

Acknowledgement—Part of the numerical results have been achieved by L. Gommert and D. Werde while working for their Diploma degree.

Discussion of results with Dr.-Ing. H. Schmidt-Traub and Dr.-Ing. H. Thiele are gratefully acknowledged.

REFERENCES

1. U. Plöcker and H. Schmidt-Traub, Instationärer Stofftransport zwischen einer Einzelkugel und einer ruh-

enden Umgebung, *Chemie-Ingr-Tech.* **44**, 313–319 (1972).
2. H. Brauer and D. Mewes, *Stoffaustauch einschließlich chemischer Reaktionen.* Sauerländer, Aarau (1971).
3. G. Carrubba, Untersuchung des instationären Stoffstransportes in Kugeln mit innerer Zirkulation. Internal unpublished report.
4. R. Kronig and J. C. Brink, On the theory of extraction from falling droplets, *Appl. Scient. Res.* **A2**, 142–154 (1950).
5. H. Schmidt-Traub, final report on the research project: Instationärer Stofftransport an festen Partikeln, Tropfen und Blasen. Unpublished report.

TRANSFERT MASSIQUE INSTATIONNAIRE A TRAVERS L'INTERFACE DE PARTICULES SPHERIQUES—2^e PARTIE: DISCUSSION DES RESULTATS OBTENUS PAR VOIE THEORIQUE

Résumé—Les équations aux dérivées partielles données dans la première partie sont traitées par voie numérique et les résultats sont discutés. On considère d'abord le transfert massique à travers l'interface sans mouvement dans chaque phase en se limitant à la concentration moyenne dans la sphère et aux nombres de Sherwood moyens pour les phases. On présente des équations empiriques pour la concentration moyenne dans la sphère dans les cas limites d'une résistance au transfert dans une seule des deux phases.

L'article considère ensuite l'influence de la convection sur le transfert massique. Pour une résistance au transfert massique dans la sphère, il existe une limite supérieure du nombre de Sherwood moyen qui est due au fait que lignes de courant dans la sphère deviennent des lignes de concentration constante. Le nombre de Sherwood instantané change par échelon en fonction du temps, ce qui peut s'expliquer par le mouvement du fluide dans la sphère. Dans le second cas limite d'une résistance au transfert dans le fluide environnant, le nombre de Sherwood est étudié en fonction des nombres de Fourier, de Henry et de convection.

INSTATIONÄRE MASSENÜBERTRAGUNG DURCH DIE GRENZSCHICHT KUGELIGER TEILCHEN TEIL II—DISKUSSION DER THEORETISCH ERMITTELTEN ERGEBNISSE

Zusammenfassung—Der zweite Teil der Untersuchung ist einer ausführlichen Diskussion der Ergebnisse gewidmet, die durch numerische Lösung der Differentialgleichungen für den Stofftransport durch die Grenzfläche kugelförmiger Partikeln erhalten wurden. Als erstes wird der Fall behandelt, bei dem sich beide Phasen im Zustand der Ruhe befinden. Auf die mittlere Konzentration in der Partikel und die mittleren Sherwood–Zahlen für beide Phasen wird dabei eingegangen. Berechnungsgleichungen für die mittlere Konzentration in der Kugel werden für die beiden Grenzfälle, bei denen nur in jeweils einer Phase ein Stofftransportwiderstand auftritt, mitgeteilt. Im letzten Kapitel wird der Einfluß der Konvektion auf den Stofftransport diskutiert. Tritt ein Stofftransportwiderstand nur in der Partikel auf, dann ergibt sich für die mittlere Sherwood–Zahl ein oberer Grenzwert. Dieser ist darauf zurückzuführen, daß die Stromlinien innerhalb der Partikel Linien konstanter Konzentration werden. Die momentane Sherwood–Zahl ändert sich für diesen Fall im Bereich niedriger Werte der Fourier–Zahl sprungweise, was auf die Bewegung des Fluids innerhalb der Partikel zurückzuführen ist. Für den zweiten Grenzfall, für den der Stofftransportwiderstand allein in der Umgebung der Partikel liegt, wird die mittlere Sherwood–Zahl als Funktion der Fourier-, der Henry- und der Konvektions-Zahl erörtert.

НЕСТАЦИОНАРНЫЙ МАССОПЕРЕНОС ЧЕРЕЗ ПОВЕРХНОСТЬ СФЕРИЧЕСКИХ ЧАСТИЦ. ЧАСТЬ 2. ОБСУЖДЕНИЕ РЕЗУЛЬТАТОВ, ПОЛУЧЕННЫХ ТЕОРЕТИЧЕСКИМИ МЕТОДАМИ

Аннотация — Обсуждаются результаты численного решения приведенного в первой части работы дифференциального уравнения. Рассматривается перенос массы через поверхность частицы при отсутствии движения в какой-либо из фаз. Анализ проводится для средней концентрации вещества в сферической частице и среднего значения числа Шервуда для обеих фаз. Представлены эмпирические уравнения для расчета средней концентрации вещества в частице для предельного случая, когда сопротивление переносу массы оказывает только одна из фаз. В последнем разделе рассматривается влияние конвекции на перенос массы. В случае, когда сопротивление переносу массы сосредоточено только в частице, существует верхний предел среднего числа Шервуда вследствие того, что линии тока внутри сферы становятся линиями постоянной концентрации. Текущее значение числа Шервуда изменяется скачкообразно со временем, что можно объяснить движением жидких элементов в сфере. В случае, когда сопротивление переносу массы сосредоточено только в окружающей частицу жидкости, среднее значение числа Шервуда зависит от критерия Фурье, Генри и конвективного числа.